Quasar Accretion Disk Tomography

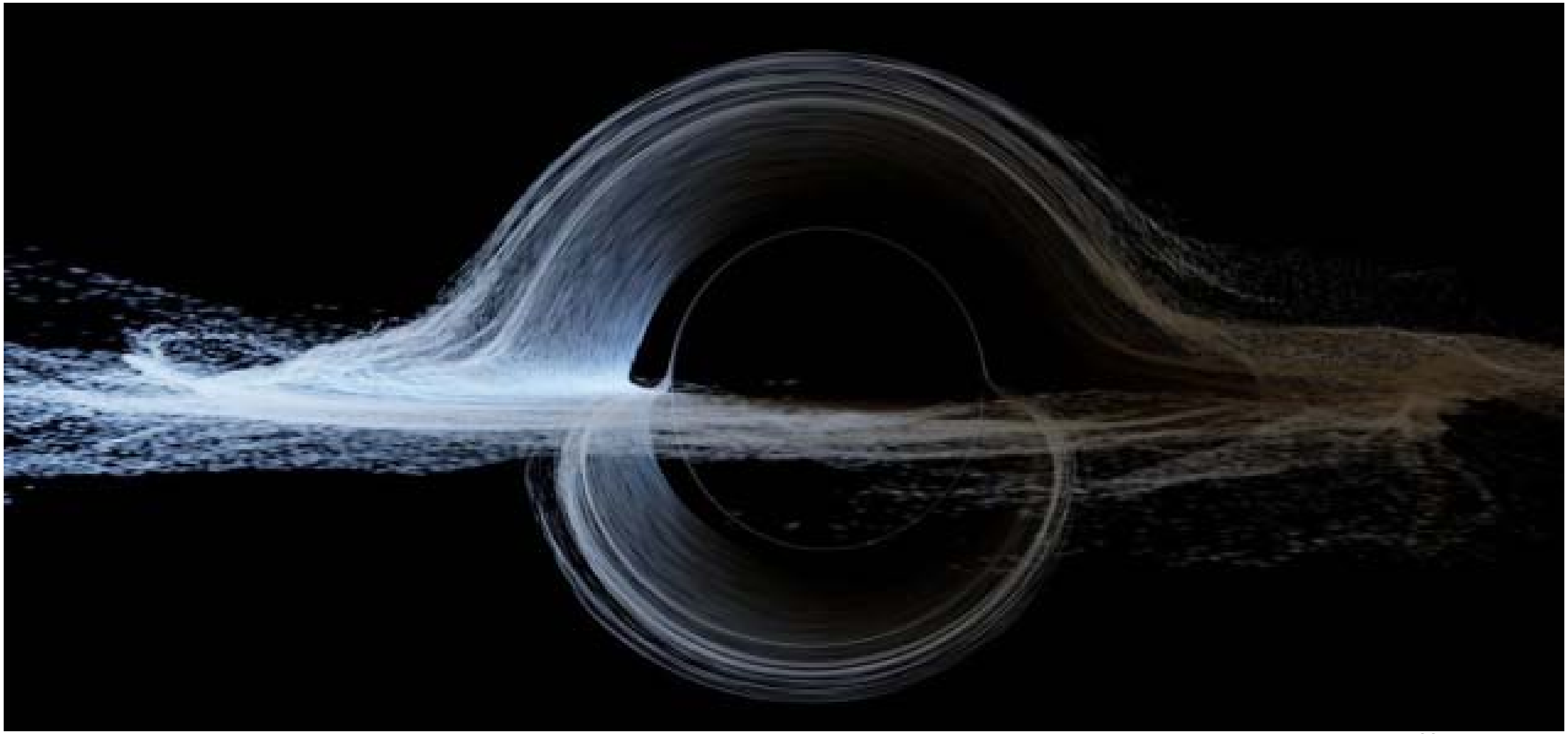

Interstellar: Kip Thorne and Double Negative visual-effects team

George Chartas (CofC)

Confronting MHD Theories of Accretion Disks with Observations, Feb 9, 2017

COLLEGE of CHARLESTON

In collaboration with:

Chris Kochanek (OSU)

Henric Krawczynski (WUSTL)

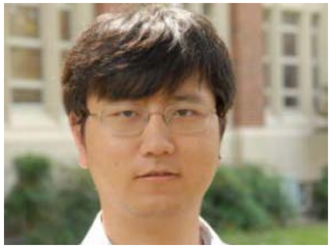

Xinyu Dai (OU)

Ana Mosquera (USNA)

Christopher Morgan (USNA)

Lukas Zalesky (CofC)

COLLEGE of CHARLESTON

Outline

- Accretion Flows and Coronae of AGN
- Microlensing used for indirect mapping of accretion disk
- Constraints on Corona Size
- Monitoring of Lensed Quasars
- Fe Kα microlensing
- Constraints on inclination, ISCO, and spin

COLLEGE of CHARLESTON

Numerical Simulations of Accretion Flows

- (Radiatively Inefficient Accretion Flows) **RIAF**

$L < 0.001\, L_{Edd}$ e.g. Sadowski+ 2016

- Radiatively Efficient Flows result in a **Thin Disk**

$0.001 L_{Edd} < L < L_{Edd}$ e.g. Noble+ 2011; Kulkarni+ 2011; Penna+ 2012; Sadowski+ 2016.

- super-Eddington accretion disks (**Slim Disks**)

$L > L_{Edd}$

COLLEGE of CHARLESTON

Numerical Simulations of Accretion Flows

GRMHD simulations for $M_{BH} = 10M_{\odot}$, $L=0.1L_{Edd}$, Schnittman+2013

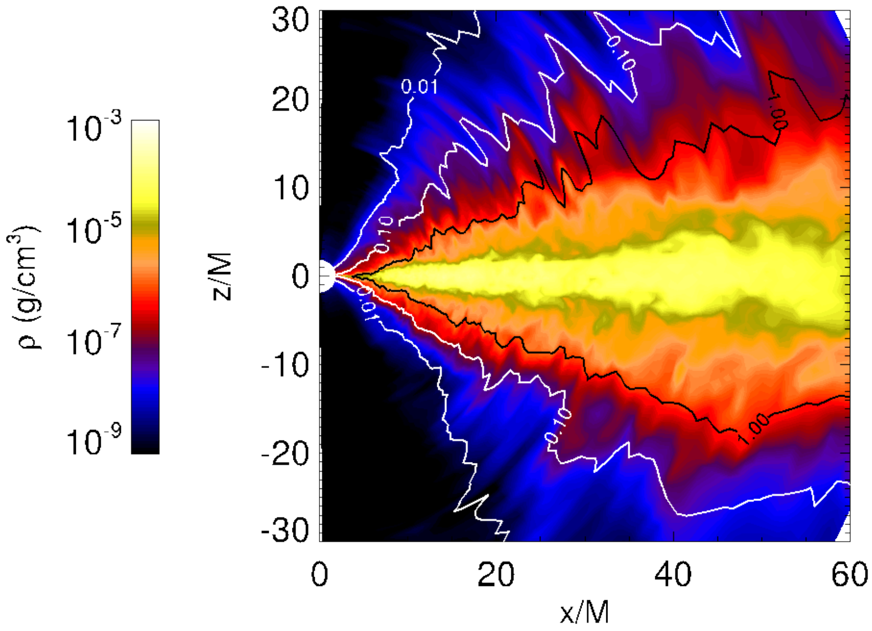

Fluid density profile

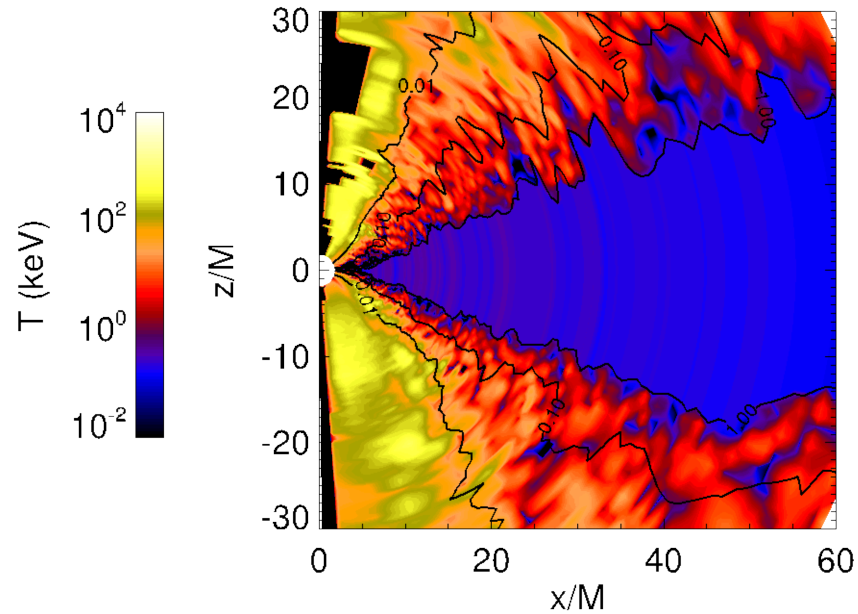

Electron temperature in the Corona

Fiducial Model

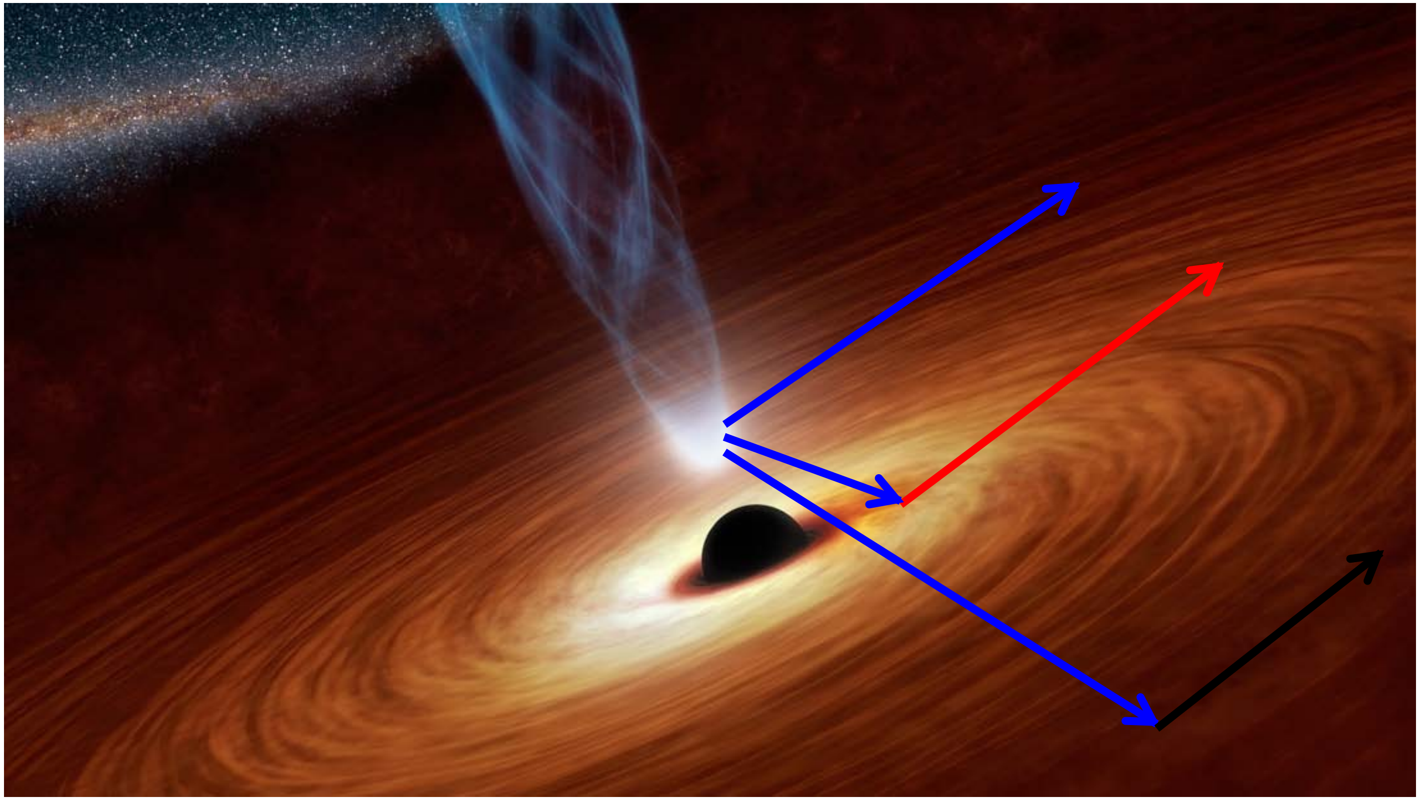

X-ray Power-Law
from compact corona

Relativistically
Blurred Reflection
(line + continuum)

Distant Reflection
(line + continuum)

Geometrically thin, optically thick accretion disk emitting primarily in UV/Optical

Quasar Accretion Disk Tomography

Direct imaging of quasars using submm VLBI is not possible due to their large distances. Microlensing, however, can resolve:

Structure of AGN Accretion Disks

- The sizes of the Optical and UV regions of AGN
- Comparison with Thin Disk Theory
- Use the distribution of shifts of the Fe line to infer the ISCO, *a*, and *i*

Structure of AGN Coronae

- The sizes of X-ray emitting coronae of AGN

COLLEGE *of* CHARLESTON

Quasar Accretion Disk Tomography

Microlensing is the bending of light produced by the individual stars in the lensing galaxy.

Microlensing variability occurs when the complex pattern of caustics produced by stars in the lens moves across the source plane.

The characteristic scale of these caustic patterns is the **Einstein radius.**

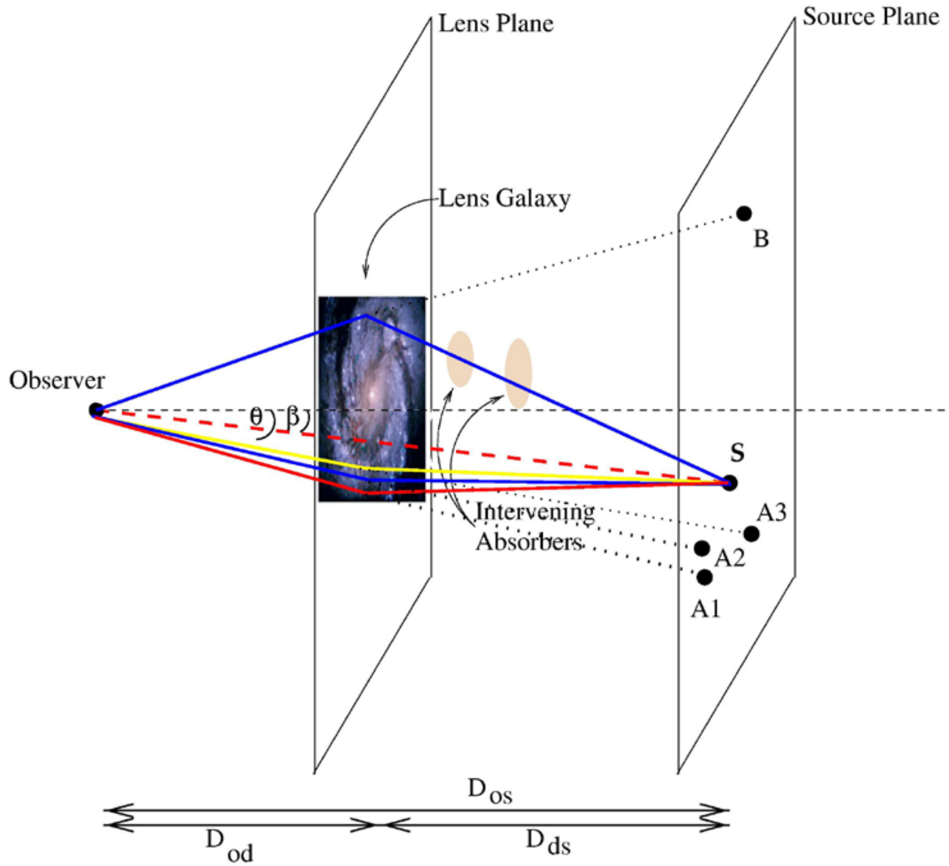

Conceptual diagram of the deflection of light in a 4 image gravitational lens system.

COLLEGE of CHARLESTON

Quasar Accretion Disk Tomography

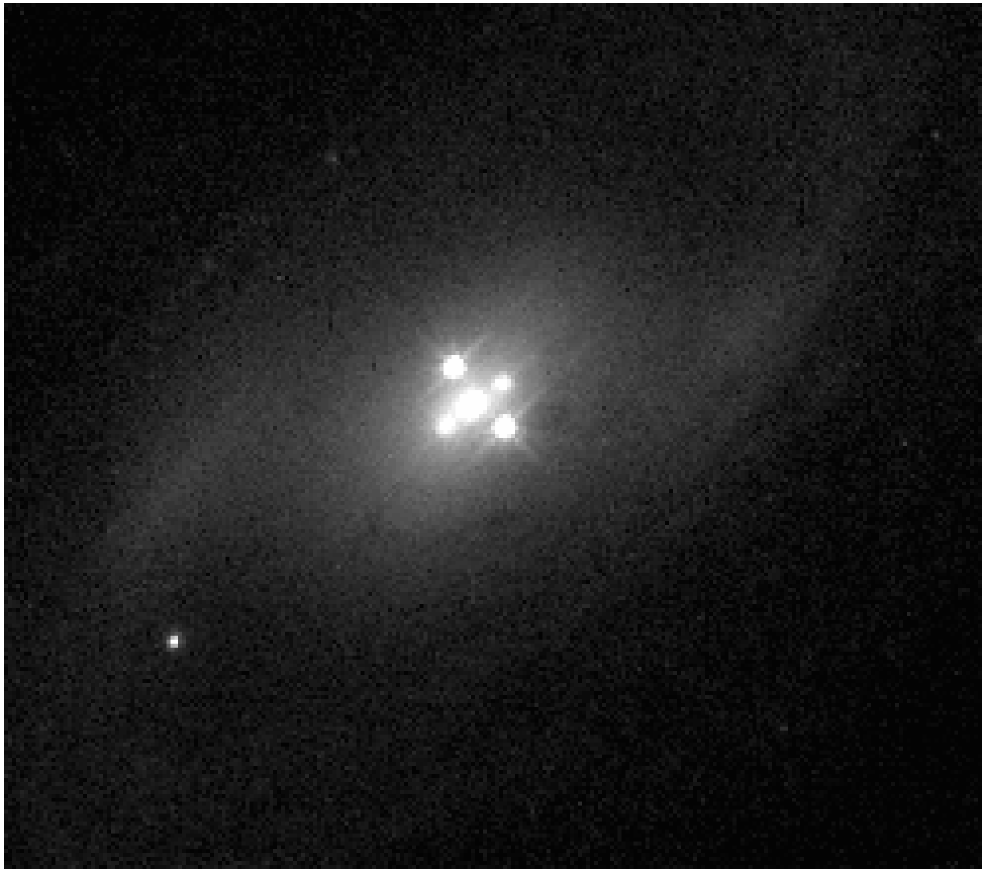

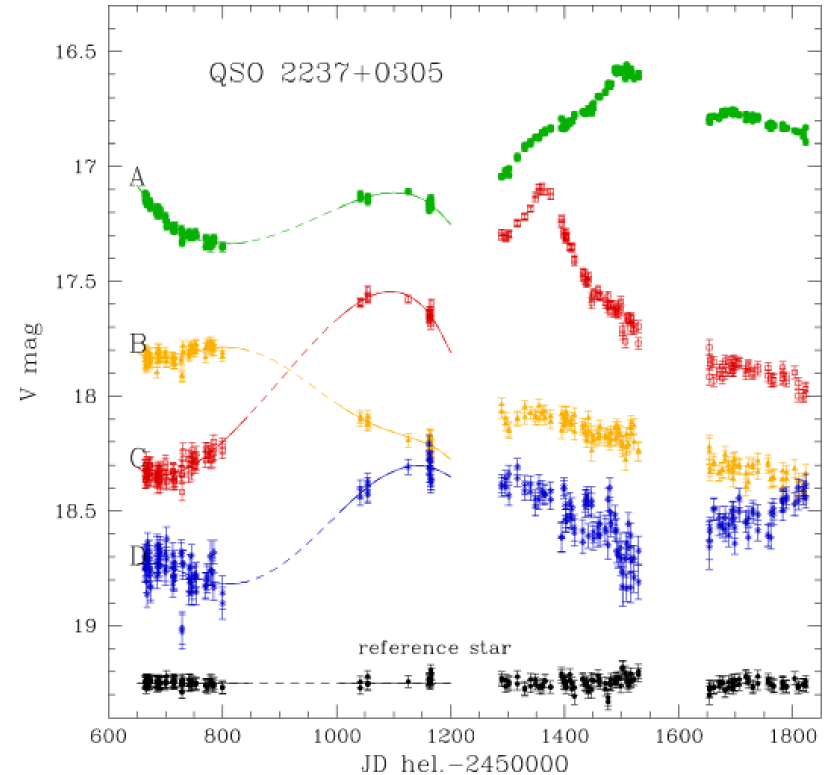

Light curves of the lensed images of QSO 2237+0305. Figure from the The Optical Gravitational Lensing Experiment (OGLE) monitoring of QSO 2237+0305; Udalski et al. 1999

COLLEGE of CHARLESTON

Quasar Accretion Disk Tomography

Microlensing Model

- The main free parameters of a microlensing model are :

- the scale lengths of the emission regions,
- a microlens mass scale,
- a mass fraction of the local surface density comprised of stars, and
- a velocity vector describing the motion of the AGN regions across the microlensing caustics.

- The microlensing analysis includes the creation of many random realizations of the star fields near each image and the generation of magnification maps.

- Dynamic Microlensing

- Simulations that allow for movement of the stars between epochs also provide constraints on the inclination of the accretion disk and the direction of motion of the caustics

COLLEGE of CHARLESTON

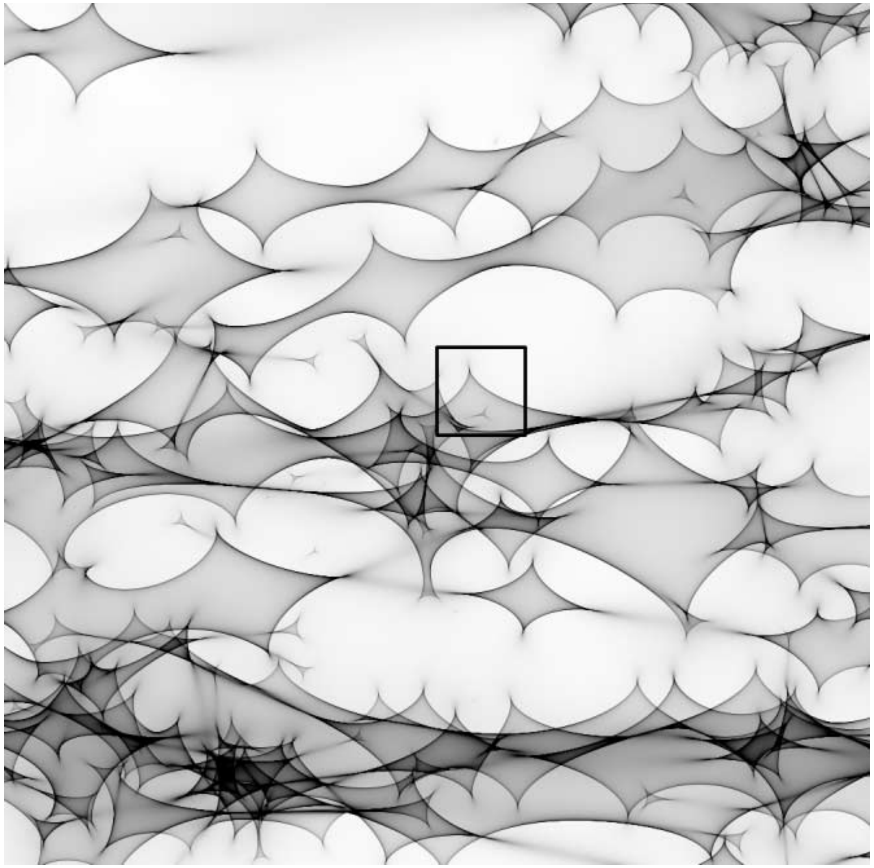

Simulated magnification map of image B of RXJ 1131 (Dai et al. 2010)

Microlensing map of QSO 2237+0305A image

COLLEGE *of* CHARLESTON

Quasar Accretion Disk Tomography

- We are performing multiwavelength monitoring of several quasars :

RX J1131-1231 ($z_s = 0.66$, $z_l = 0.30$)
Q J0158-4325 ($z_s = 1.29$, $z_l = 0.317$)
SDSS0924+0219 ($z_s = 1.524$, $z_l = 0.39$)
Q 2237+030 ($z_s = 1.60$, $z_l = 0.04$)
HE 0435-1223 ($z_s = 1.689$, $z_l = 0.46$)
PG 1115+080 ($z_s = 1.72$, $z_l = 0.31$)
SDSS1004+4112 ($z_s = 1.734$, $z_l = 0.68$)
QSO 1104-1805 ($z_s = 2.32$, $z_l = 0.73$)

with the main scientific goal of measuring the emission structure near the black holes in the optical\UV and X-ray bands in order to test accretion disk models.

- X-ray monitoring observations were performed with *Chandra*
- *Optical* (*B*, *R* and *I* band) observations were made with the SMARTS Consortium 1.3m telescope in Chile.

COLLEGE of CHARLESTON

Quasar Accretion Disk Tomography

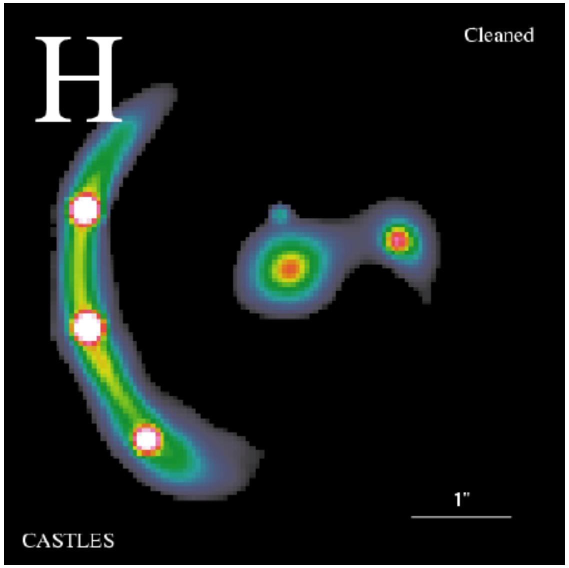

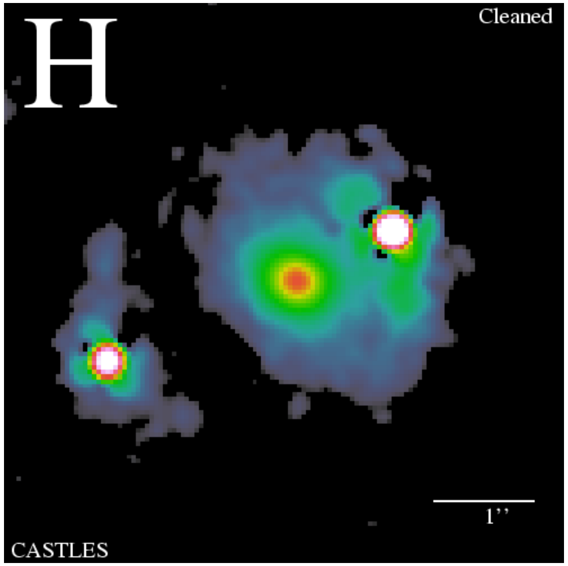

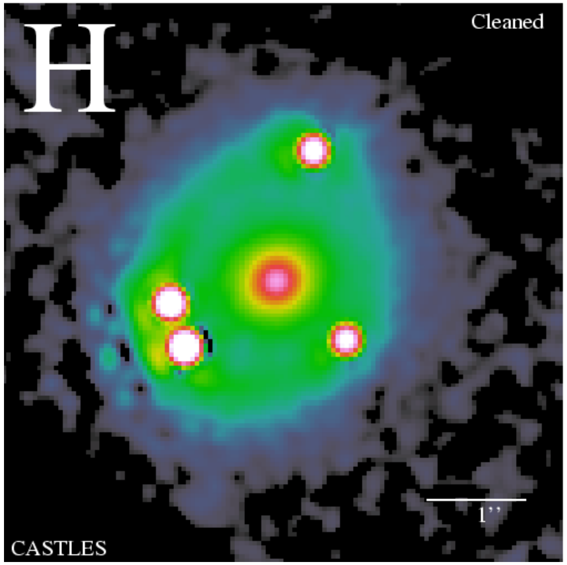

A HST image of quasar
RX J1131-1231
z_s = 0.658, z_l=0.295

A HST image of quasar
HE 1104-1805
z_s = 2.32 , z_l = 0.73

A HST image of quasar
PG 1115 +080
z_s = 1.72 , z_l = 0.31

COLLEGE of CHARLESTON

Monitoring of RX J1131-1231 with Chandra

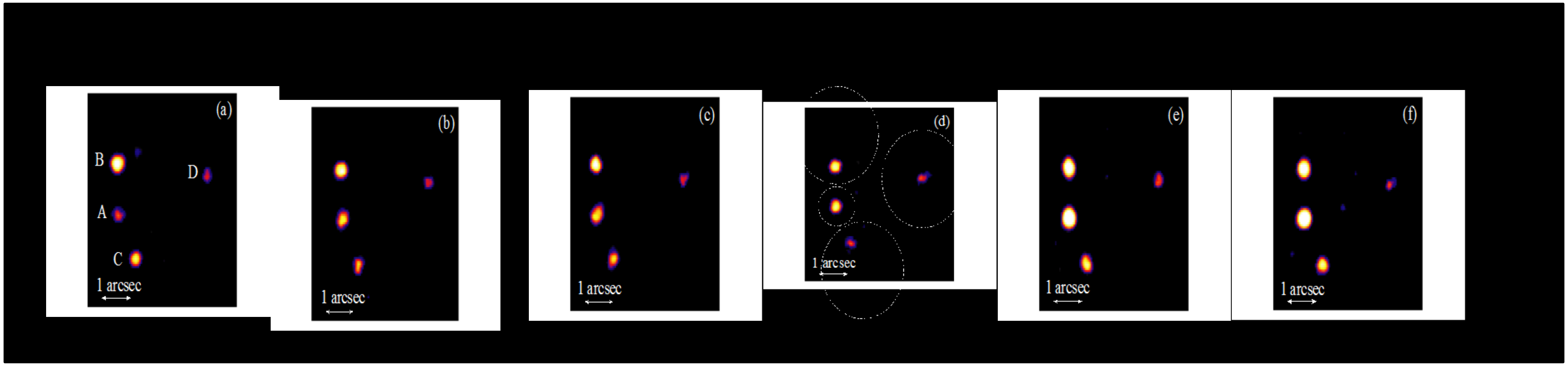

Images in the 0.2 - 10 keV bandpass of the *Chandra* observations of RX J1131-1231.

Data taken between April 4, 2004 & July 1, 2014.
38 pointings, between 4-28 ksec each.

Constraints on Accretion Disk Size from Microlensing

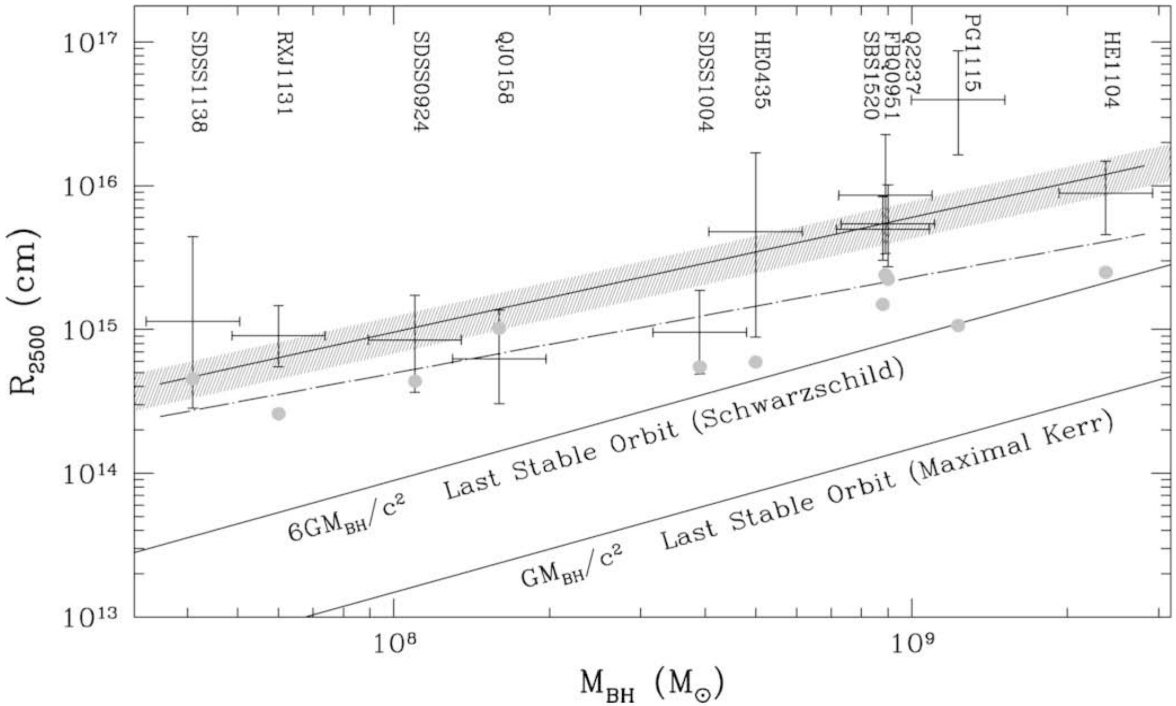

The Quasar Accretion Disk Size versus Black Hole Mass Relation Morgan et al. 2010

Thin accretion disk theory predicts that the characteristic size of the accretion disk at wavelength λ scales as

$$R_\lambda = (9.7\times10^{15})(\lambda/\mu m)^{4/3}(M_{BH}/10^9 M_{solar})^{2/3}(L/\eta L_E)^{1/3}\ cm$$

and the disk temperature scales as: $T_{eff} \propto r^{-\beta},\ \beta = 3/4$

COLLEGE of CHARLESTON

Constraints on Corona Size from Microlensing

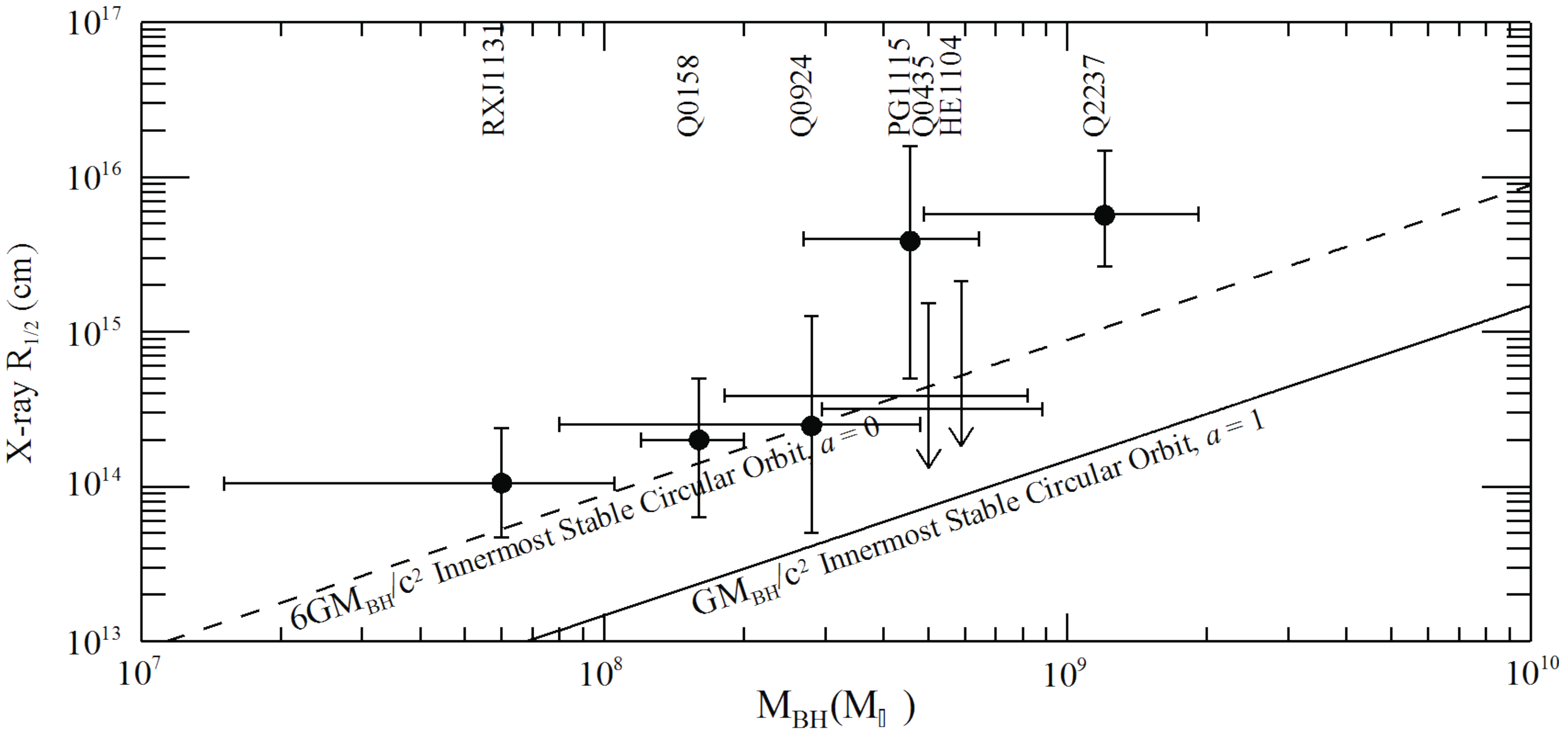

X-ray half-light radii of quasars as determined from our microlensing analysis versus their black hole masses.

Chartas et al. 2016

COLLEGE of CHARLESTON

Evidence for Microlensing

0.2 – 10 keV light-curves of RXJ1131

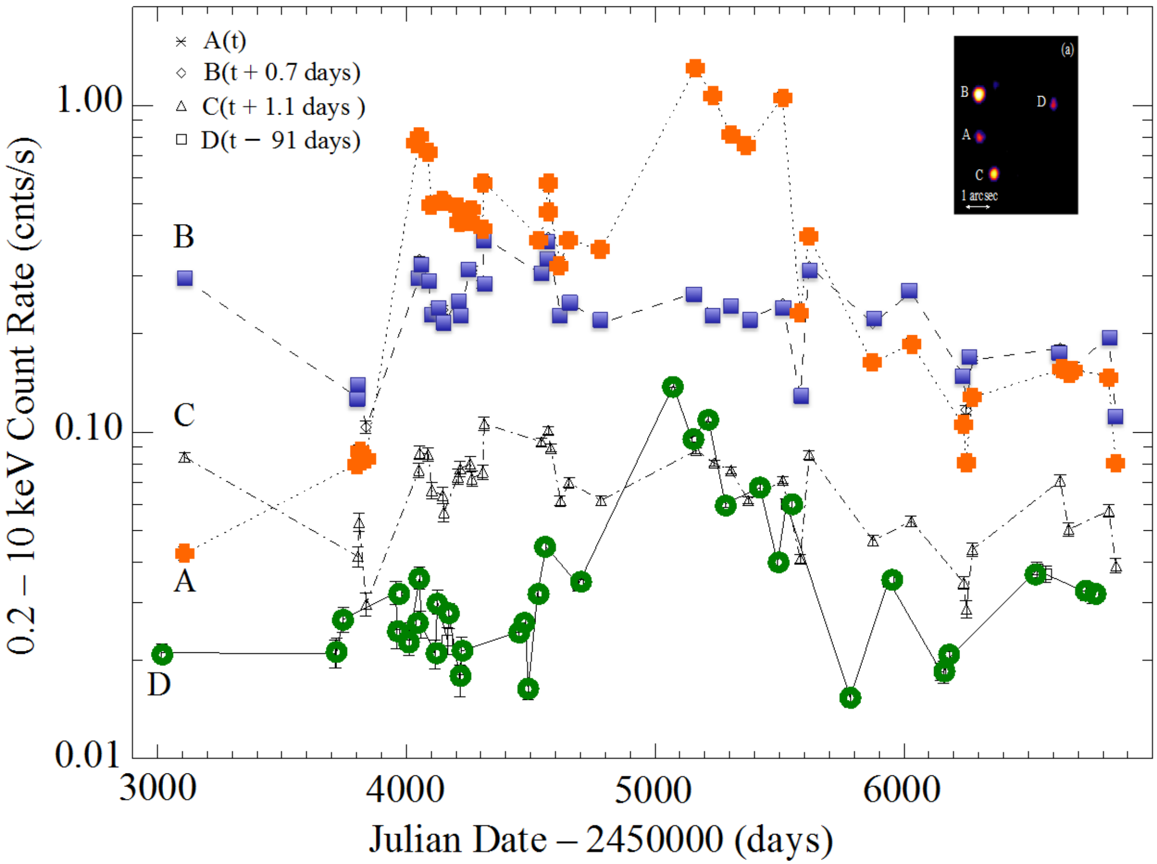

Large uncorrelated varibility detected in images A and D imply large microlensing events in these images.

COLLEGE of CHARLESTON

Evidence for Microlensing in all Images of RXJ1131

Shifted Fe Kα line in Spectrum of image D (4/23/2008)

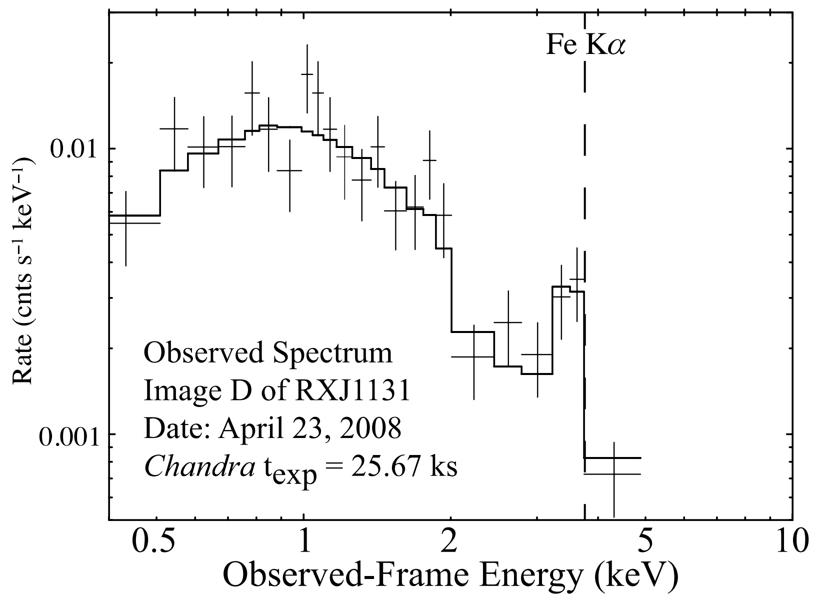

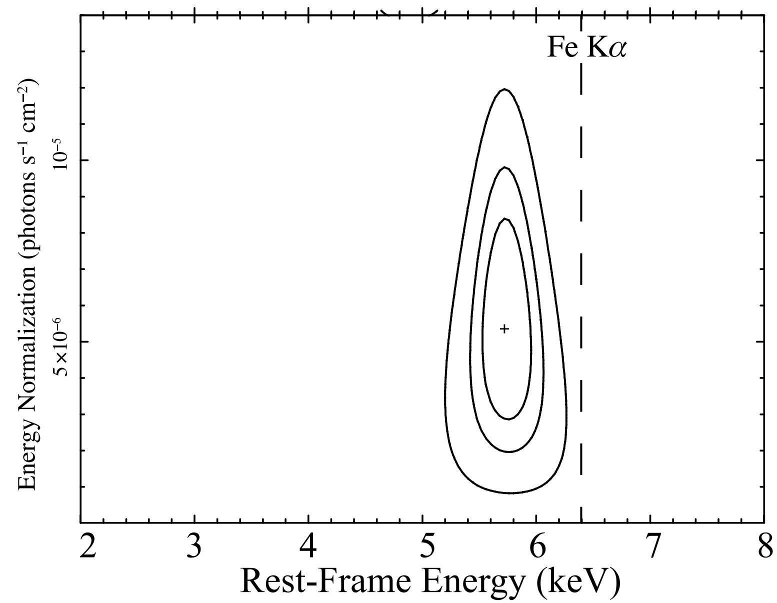

- 4 images × 38 pointings = 152 spectra
- 58 lines (>90%CL), 18 lines (>99%CL)

COLLEGE of CHARLESTON

Evidence for Microlensing in all Images

Monte Carlo simulations to test significance of Fe lines

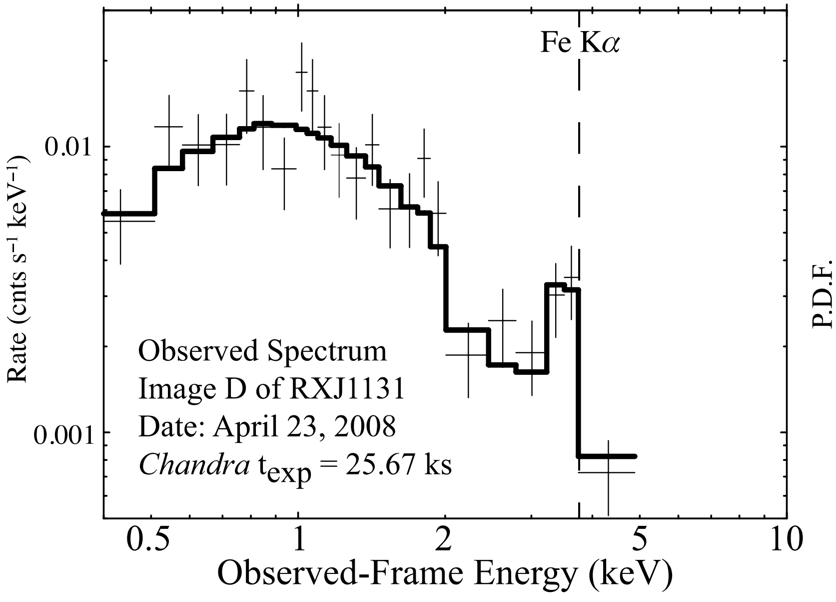

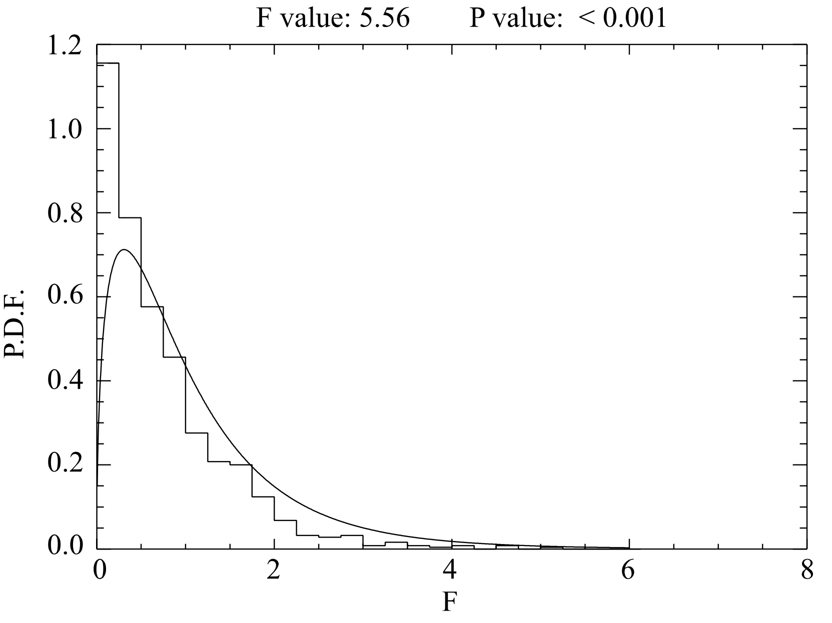

COLLEGE of CHARLESTON

Evidence for Microlensing in all Images

Shifted Fe Kα line in Spectrum of image B (1/1/2007)

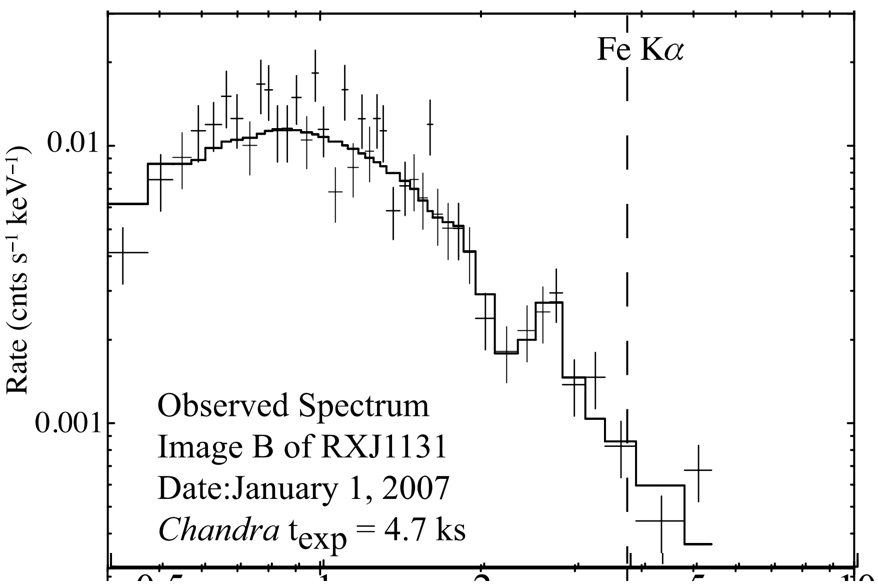

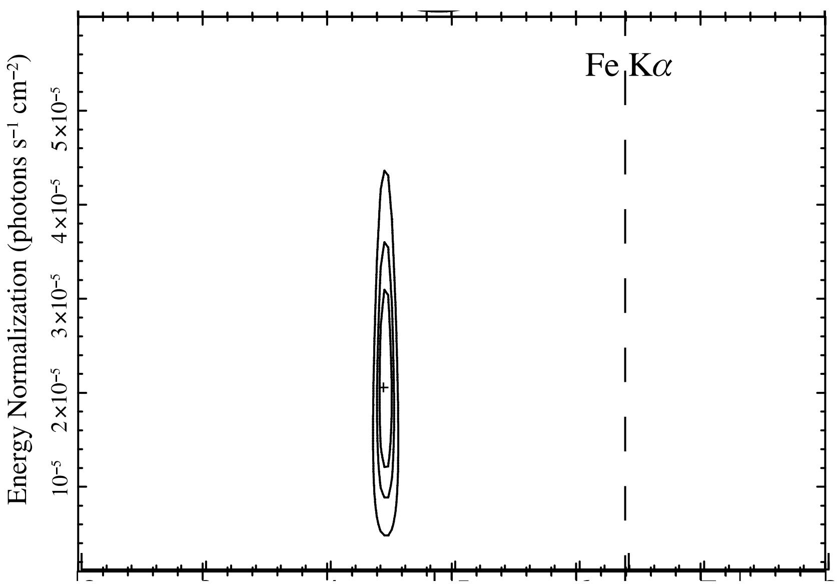

Significant spectral variability, including the centroid and equivalent width of the Fe Kα line

COLLEGE of CHARLESTON

Evidence for Microlensing in all Images

Shifted Fe Kα line in Spectrum of image A (4/17/2010)

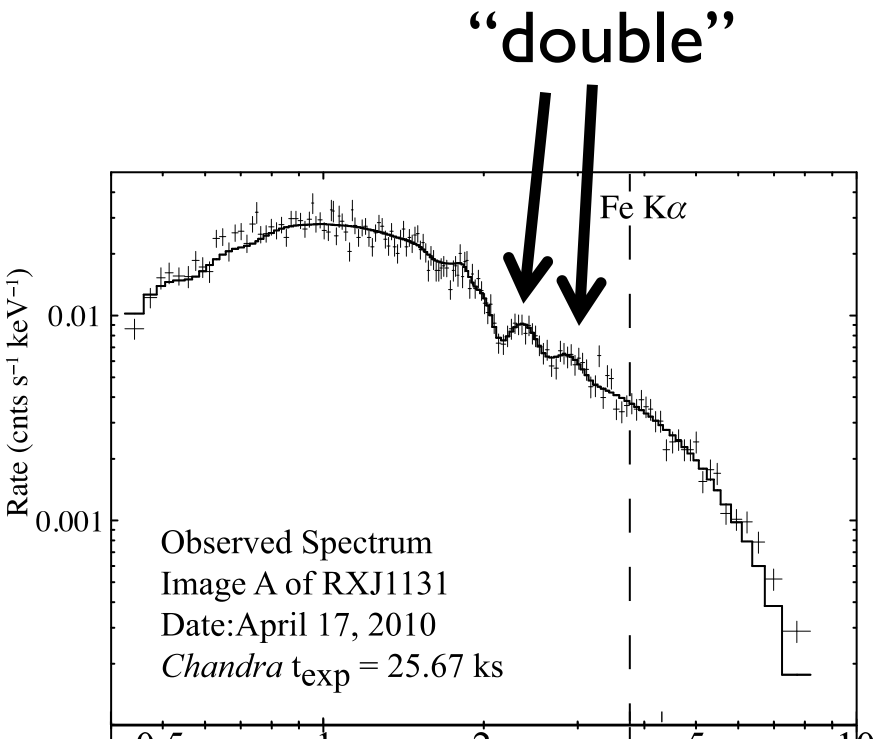

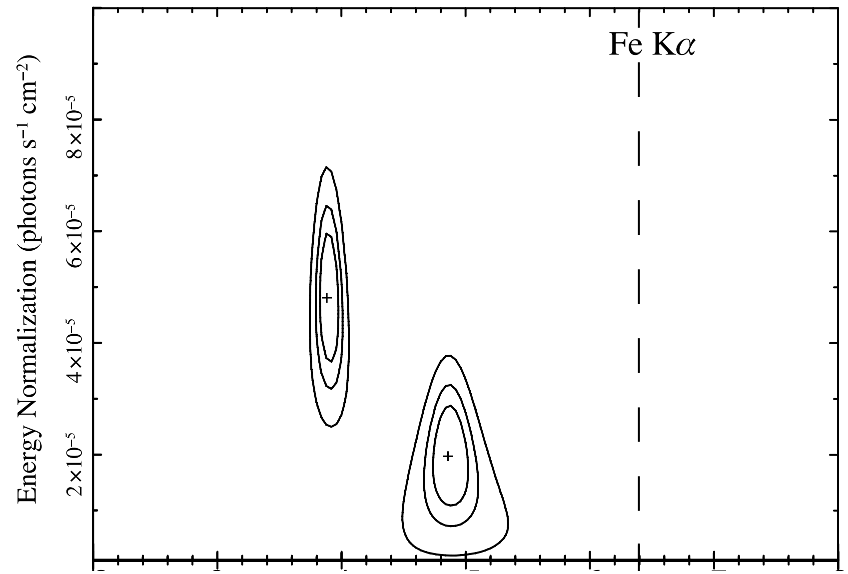

Detection of two shifted Fe Kα lines

COLLEGE of CHARLESTON

Evidence for Microlensing in all Images

Shifted Fe Kα line in Spectrum of image C (1/21/2011)

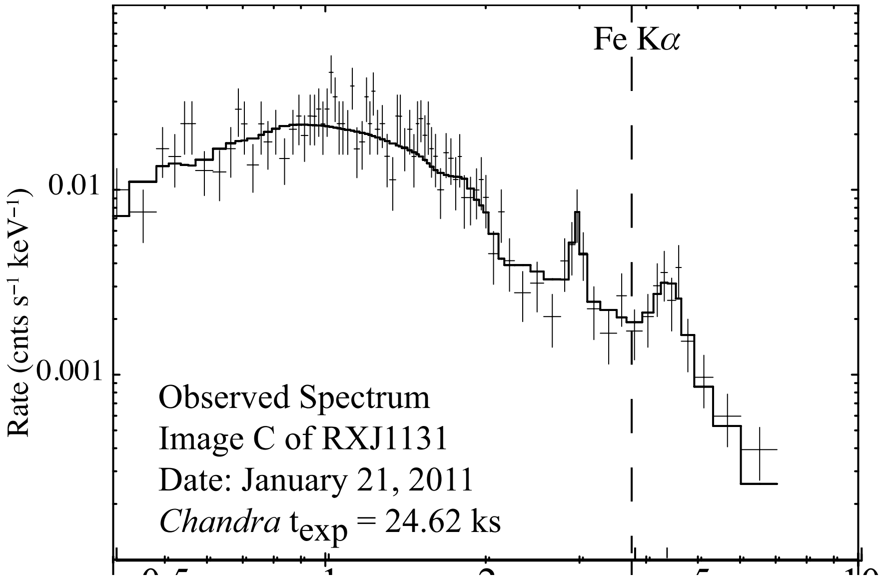

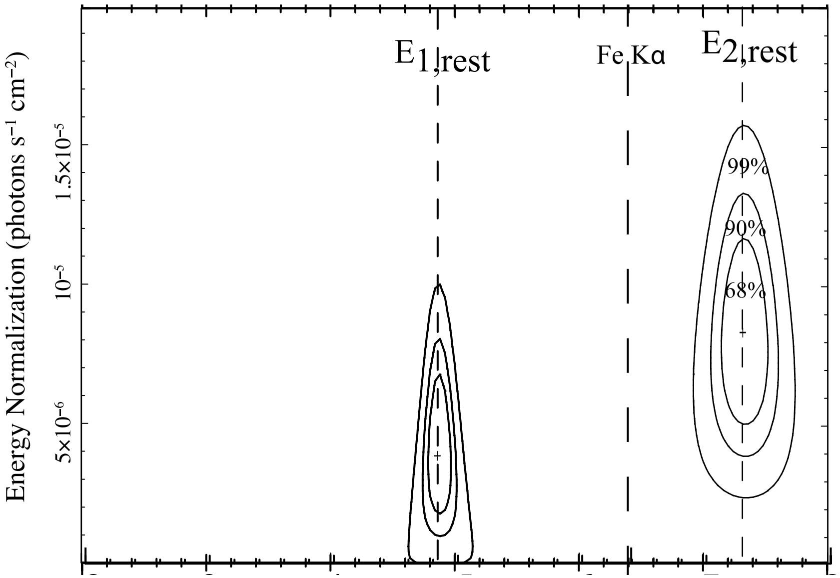

Significant changes of line centroids and equivalent widths.

COLLEGE of CHARLESTON

Intrinsic Variability of RXJ 1131 (Image C)

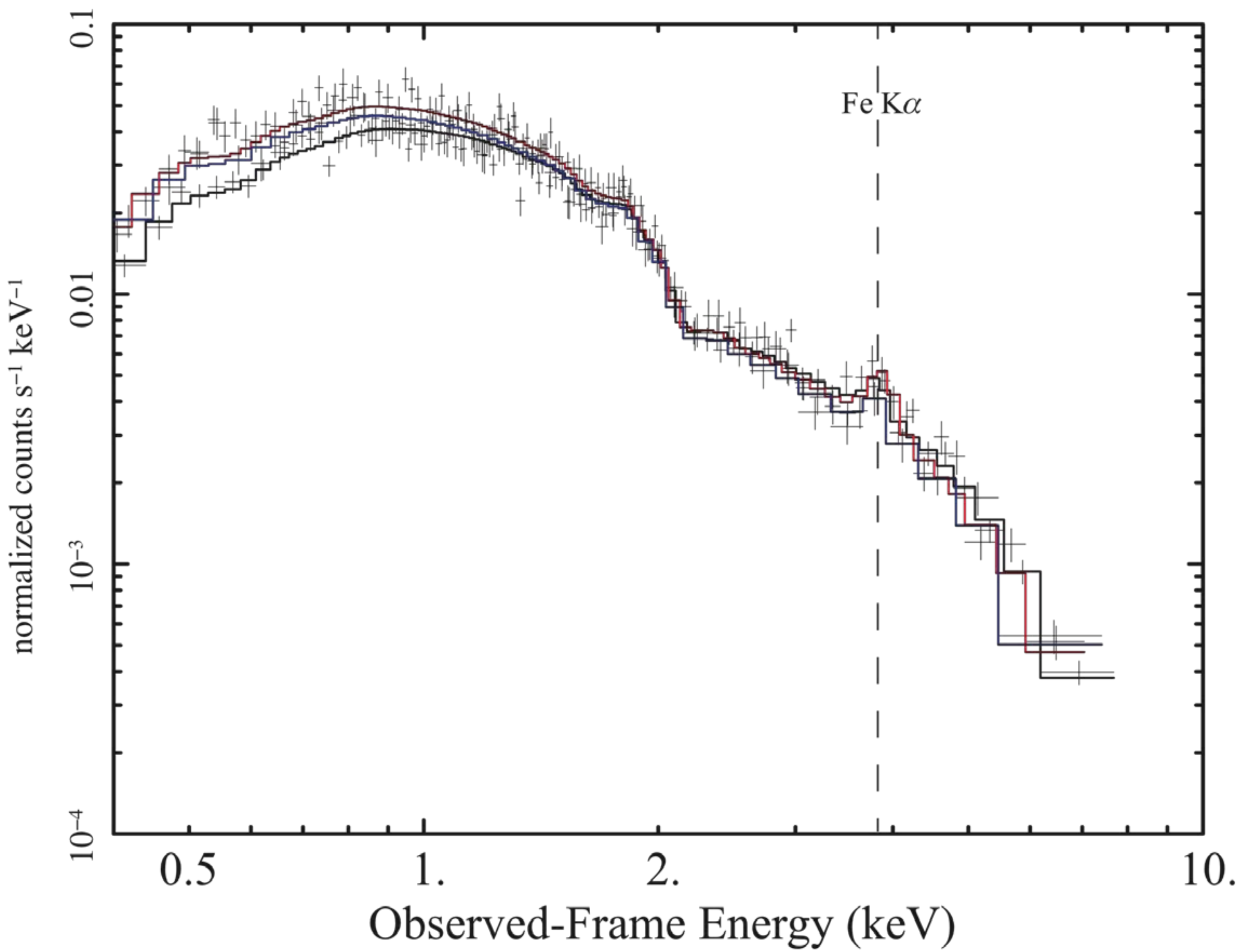

COLLEGE of CHARLESTON

Generalized Doppler Shift

The observed energy of a photon emitted near the event horizon of supermassive black hole will be shifted with respect to the emitted rest-frame energy due to general relativistic and Doppler effects.

$$g = \frac{E_{obs}}{E_{emit}} = \delta\sqrt{\frac{\Sigma\Delta}{A}}$$

Where the Doppler shift is:

$\delta = \frac{\sqrt{1-v_\phi^2}}{1-v_\phi \cos\theta_c}$, where v_ϕ is the azimuthal velocity and θ_c is the angle between our line-of-sight and the direction of motion of the emitting plasma.

A, Σ, and Δ are defined as

$$A = \left(r^2 + a^2\right)^2 - a^2\Delta \sin^2\theta,\ \Sigma = r^2 + a^2 \sin^2\theta,\ \Delta = r^2 - 2r_g r + a^2$$

COLLEGE of CHARLESTON

g-distribution method

The *g*-distribution method relies on determining the **distribution of FeKα energy shifts** from the spectra of individual lensed images obtained from a large number of X-ray observations.

The value of ***g* will range between extremal values** that depend on the inclination angle *i*, the caustic crossing angle θ_c, and the spin of the black hole.

The *g*-distribution is expected to show **sharp cut-offs**. The low energy cutoff is sensitive to the ISCO and the high energy cut-off is sensitive to the inclination angle.

Relativistic Fe Kα Method

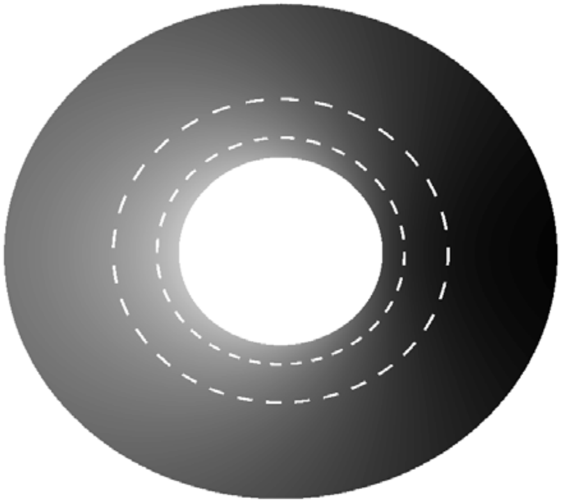

Line broadening from an intrinsically narrow line emitted from two radii in an accretion disk. The lowest panel shows the result obtained by summing many disc radii, weighted by the expected emissivity. Courtesy of Fabian et al. 2000

COLLEGE of CHARLESTON

Relativistic Fe Kα Method

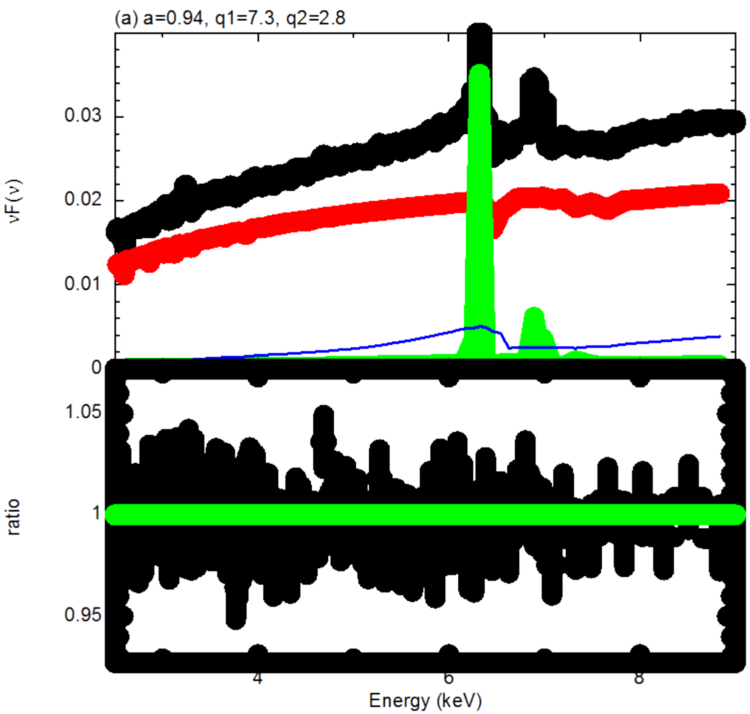

Unfolded Suzaku XIS spectrum of NGC 3783 overlaid with the best fitting relativistic Fe Ka model (top) and the associated data/model ratio (bottom). Figure from Reynolds et al. (2012).

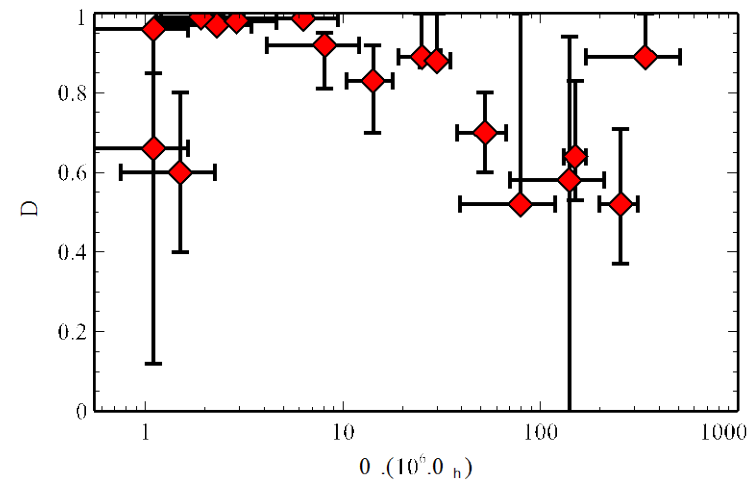

Black hole mass and spin *a* from a sample of Seyferts presented in Reynolds et al. (2013).

COLLEGE of CHARLESTON

g-distribution method for quasars

There are concerns that most of the measured spin parameters in Seyfert galaxies are found to be > 0.9. However, high spin black holes are more luminous and hence brighter for a given accretion rate, and hence will simply be more highly represented in flux limited surveys (Vasudevan et al. 2016).

We plan to use the g-distribution method to constrain the spins of quasars with M_{BH}: 6×10^7 $M_\odot$ – 2×10^9 $M_\odot$ and L_{Bol}/L_{Edd}: 0.01 – 0.7

Object	$\log(M_{\rm BH})$ $M_\odot$	$\log(R_{\rm E})$ cm	$\log(r_{\rm g})$ cm	R_E/v_e years	$10r_g/v_e$ months	v_e km/s	μ	$L_{\rm Bol}/L_{\rm Edd}$ (counts $\rm s^{-1}$)
RXJ1131	7.8	16.4	13.0	11.1	0.5	720	57	0.7
QJ0158	8.2	16.5	13.4	18.0	1.6	600	5	0.4
SDSS1004	9.3	16.4	14.5	9.4	14.5	785	70	0.01
Q2237	8.7	17.0	13.8	8.1	0.7	3890	16	0.04

COLLEGE of CHARLESTON

g-Distribution of Line Centroids of RXJ1131

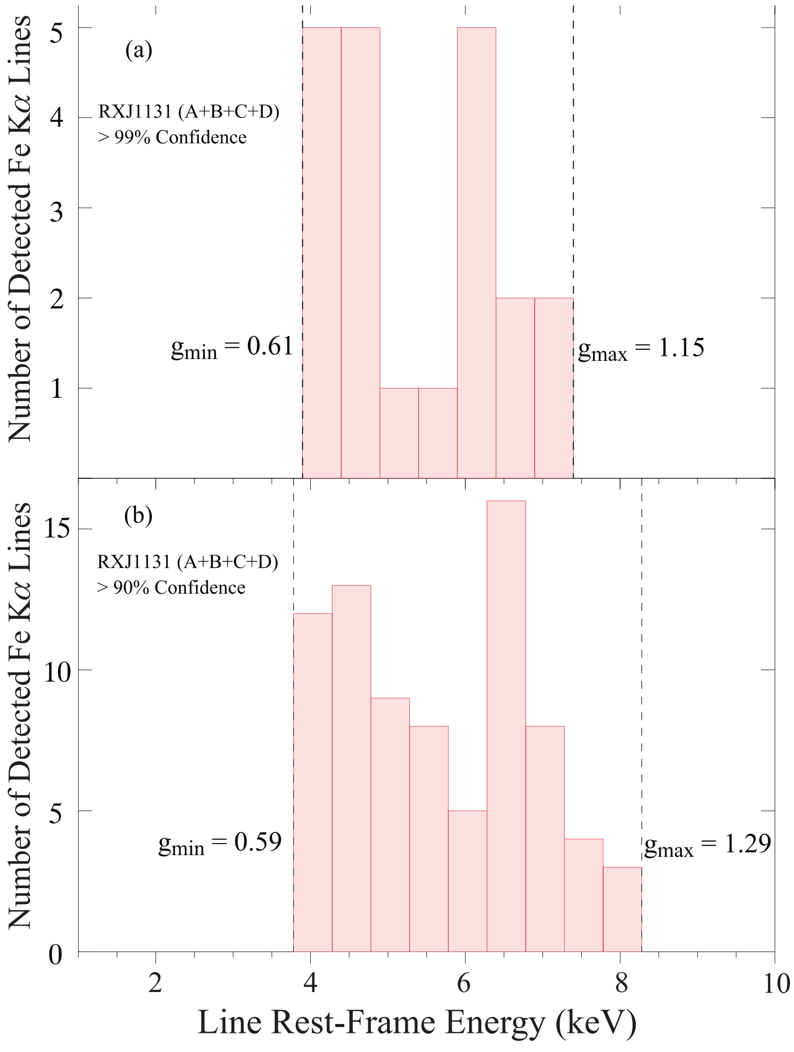

Red/blueshift: 0.61-1.15 (99% CL)

Red/blueshift: 0.59-1.29 (90% CL)

COLLEGE of CHARLESTON

g versus radius

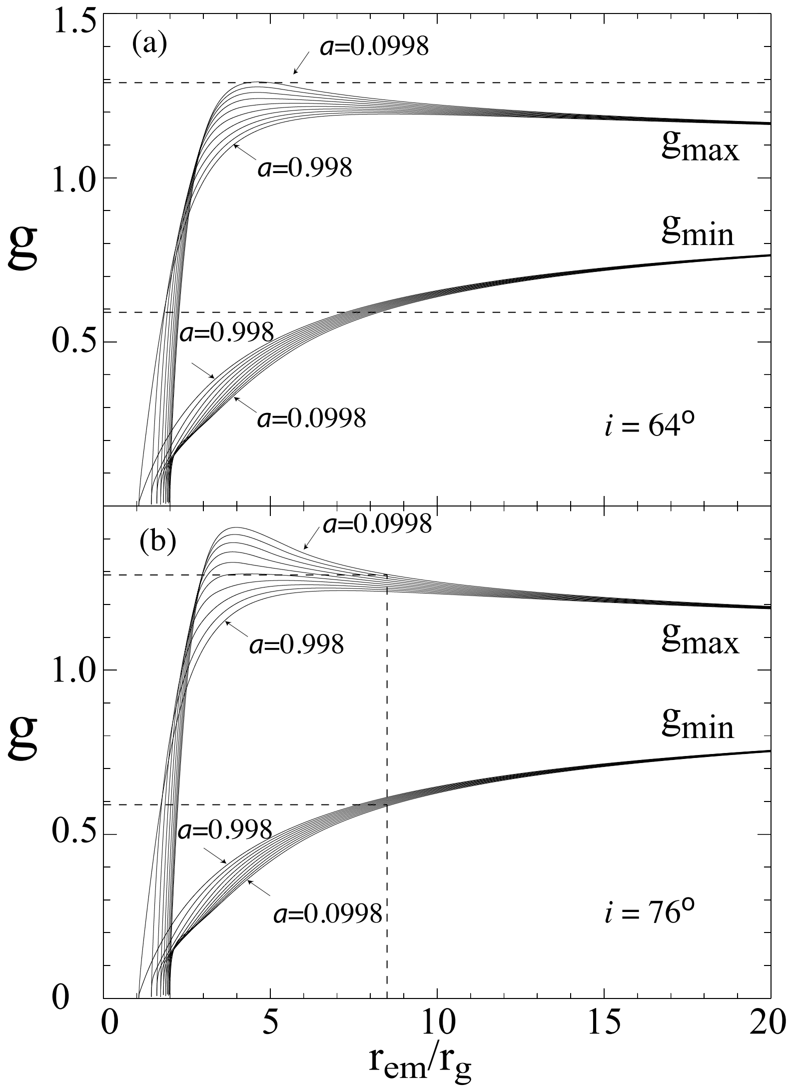

g_{max} = 1.29 ➔ $i > 64°$

g_{max} = 1.29 ➔ $i > 76°$

g_{min} = 0.59

$r_{ISCO} < 8r_g$

Assume g_{min} and g_{max} occur at same radius

COLLEGE of CHARLESTON

Numerical Simulations of Microlensing Events

(1) Modeling of the Fe-Kα emission.

- General relativistic ray tracing code (HK 2012).
- Assume ***lamppost***, wedge, or spherical corona.
- Simulate a=0, 0.1, ...0.9, 0.95, 0.98, 0.998.

(2) Modeling of Microlensing.

- Inverse ray shooting.
- Simple parameterization of magnification close to caustic fold.

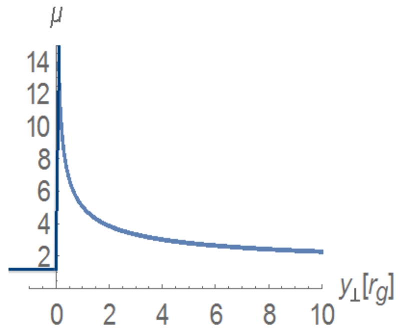

Krawczynski+ 2016

COLLEGE of CHARLESTON

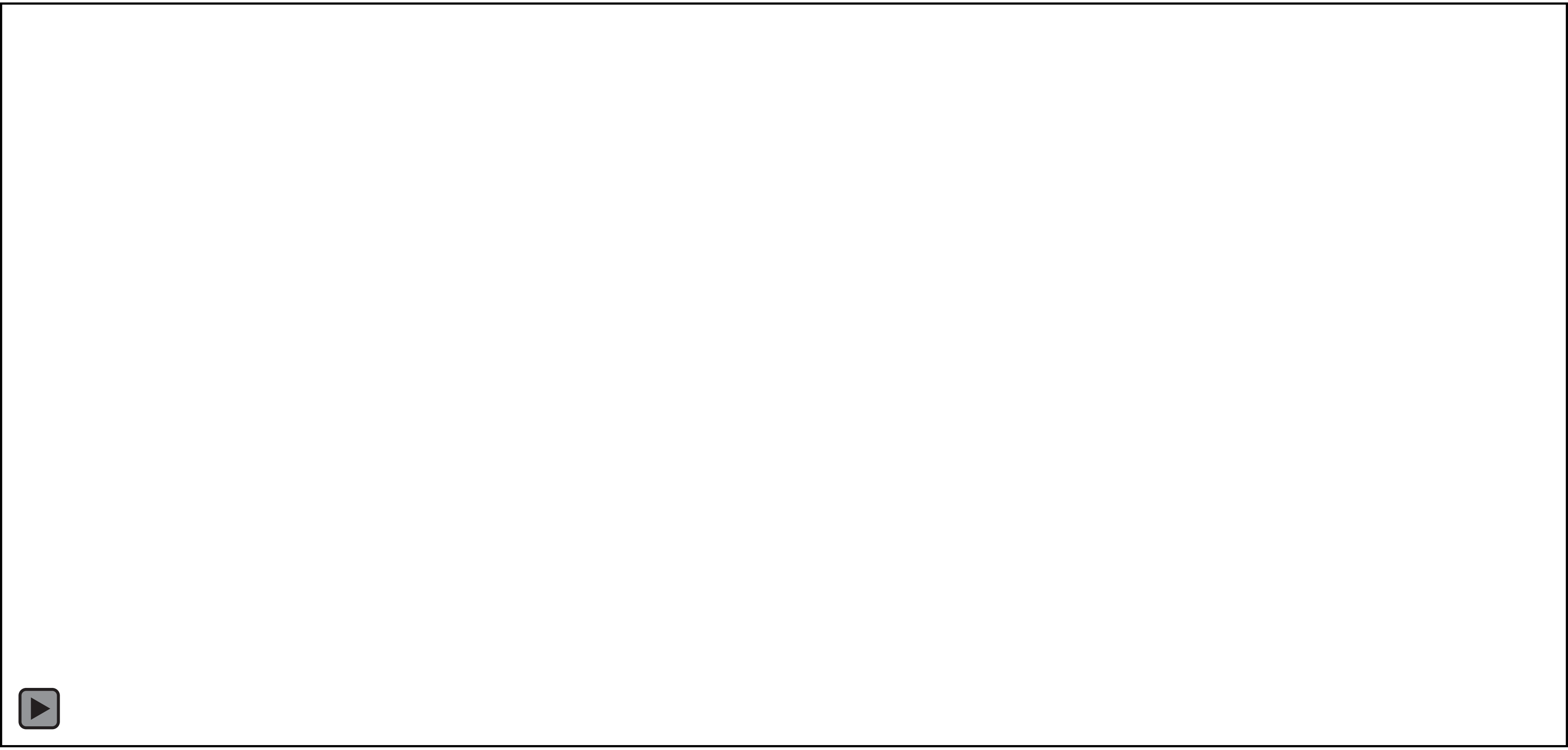

COLLEGE of CHARLESTON

Simulated g-Distribution of Line Centroids

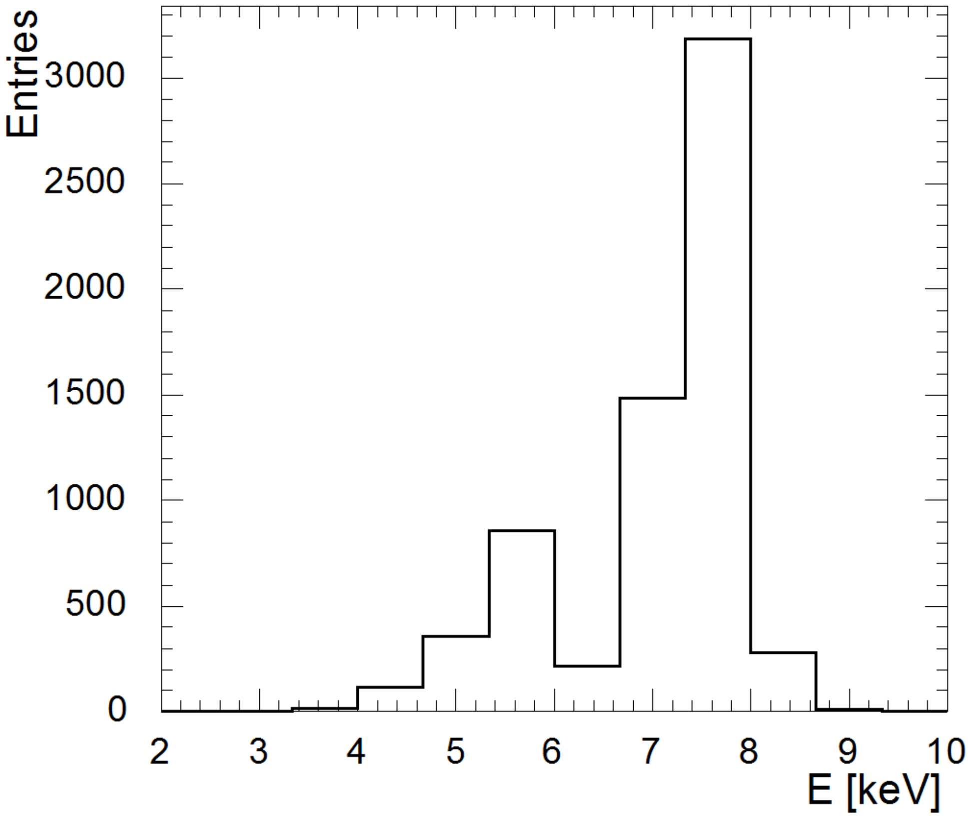

Chartas+ 2017,
Krawczynski+ 2016

Simulated distribution of the single and double peak energies for a black hole with a spin of *a* = 0.3

COLLEGE of CHARLESTON

Double Fe Kα Emission Lines (“doubles”)

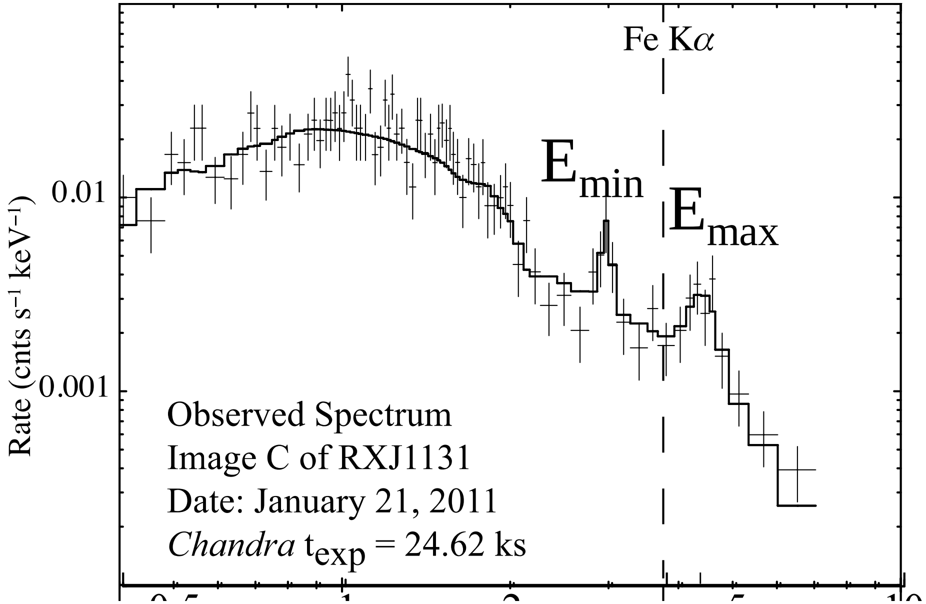

For all Images of RXJ1131

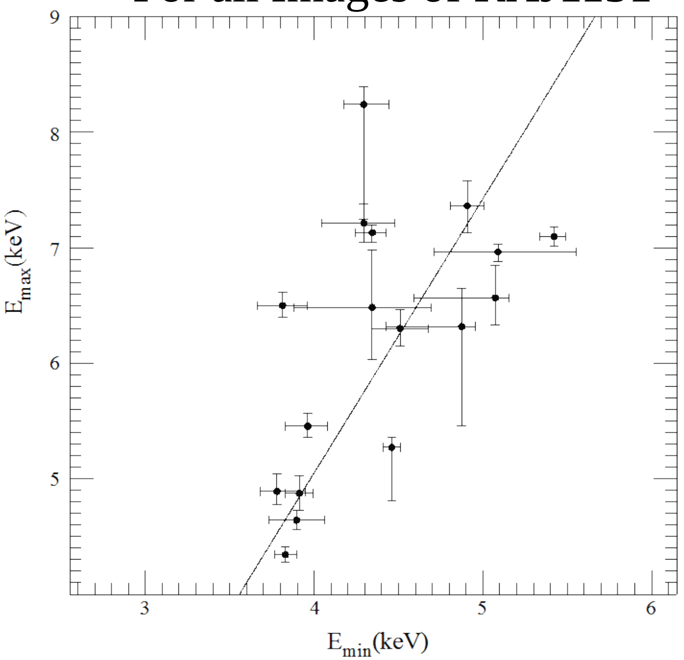

- Double peaks are reproduced in our numerical simulations.

- Moderate correlation between E_{min} and E_{max} :

For image A (Kendall’s $\tau = 0.6$, P > 98% CL)
For all images (Kendall’s $\tau = 0.4$, P > 97% CL)

COLLEGE of CHARLESTON

ΔE-distribution of doubles

Observed ΔE-distribution of RXJ1131

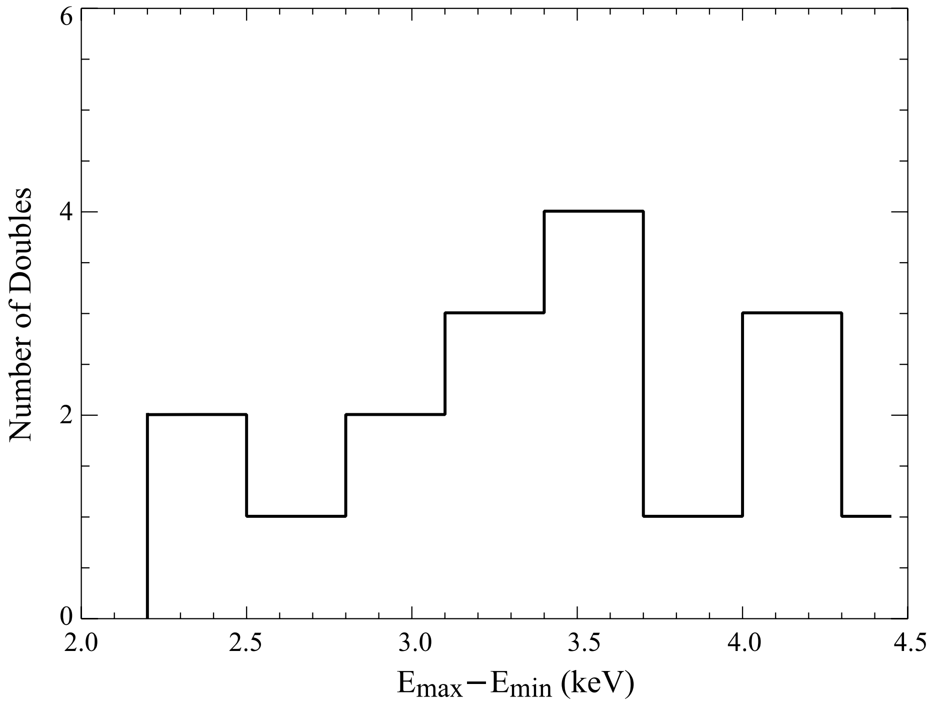

Simulated ΔE-distributions of RXJ1131

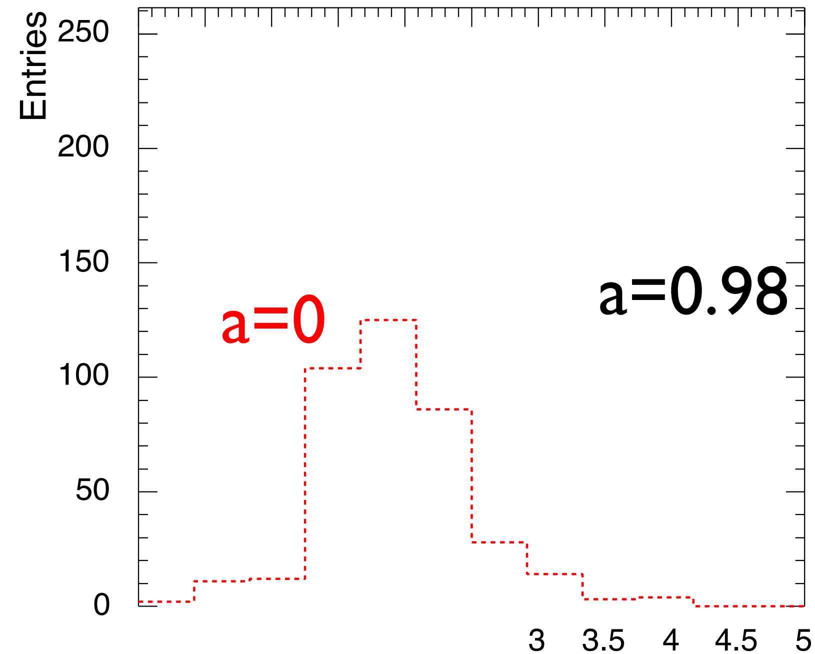

Chartas+ 2016, Krawczynski+ 2016

The distribution of energy separations of doubles depends strongly on black hole spin

COLLEGE of CHARLESTON

g **versus** Equivalent Width of shifted Fe Kα Line

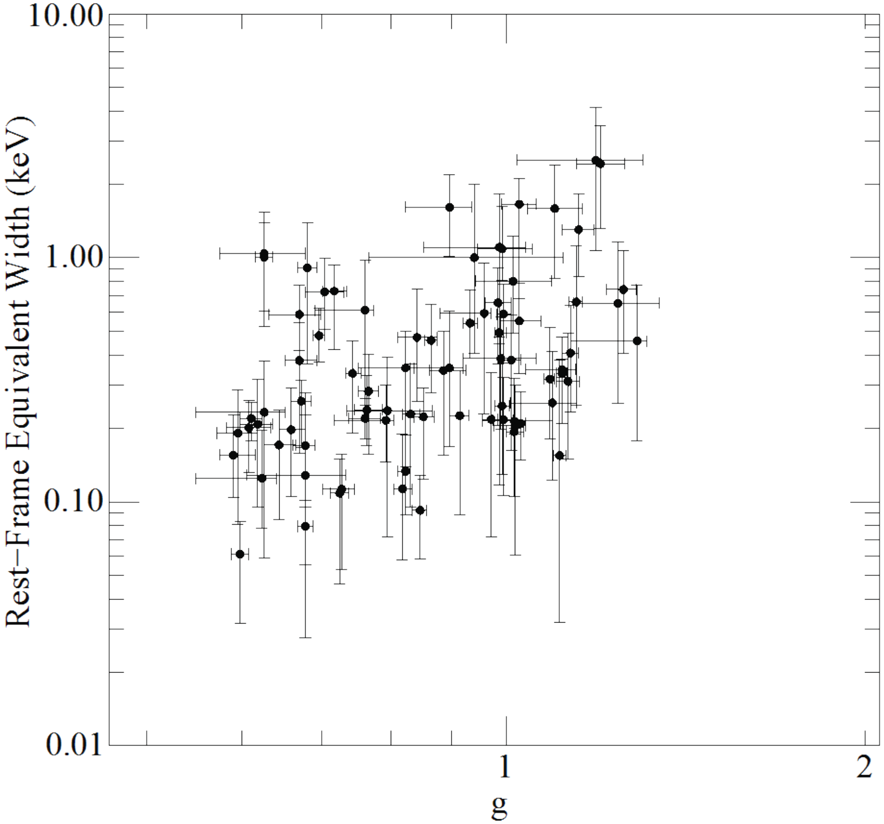

Strong correlation of *g* vs. EW
Kendall's $\tau = 0.3$, P > 99.9% CL

One possible explanation of this correlation is that blueshifted line emission is Doppler boosted resulting in the observed EW of the blueshifted lines being larger than the redshifted lines.

Supports microlensing interpretation!

COLLEGE *of* CHARLESTON

Preliminary Results for HE 0435 and Q 2237

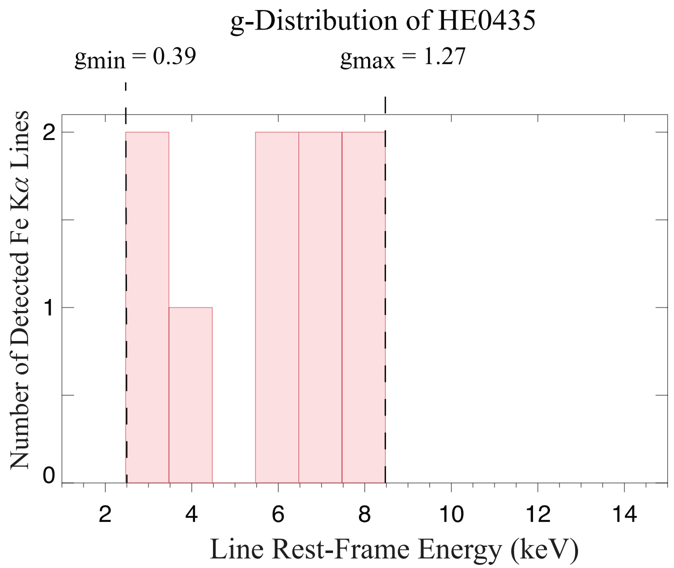

HE 0435-1223 (z_s = 1.689, z_l = 0.46)

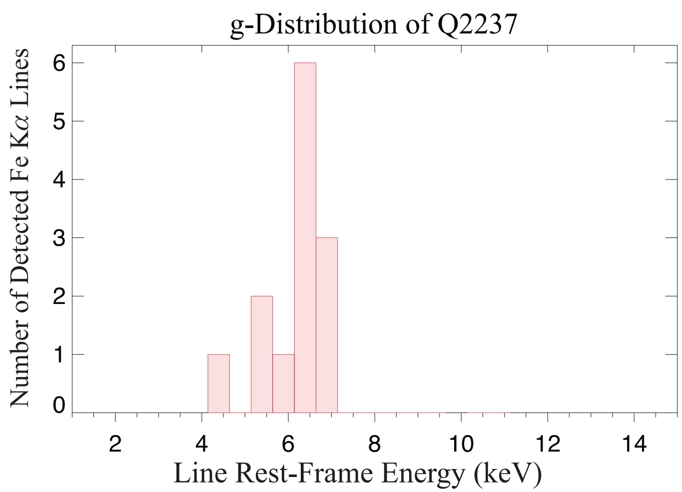

Q 2237+030 (z_s = 1.60, z_l = 0.04)

COLLEGE of CHARLESTON

Preliminary Results for HE 0435

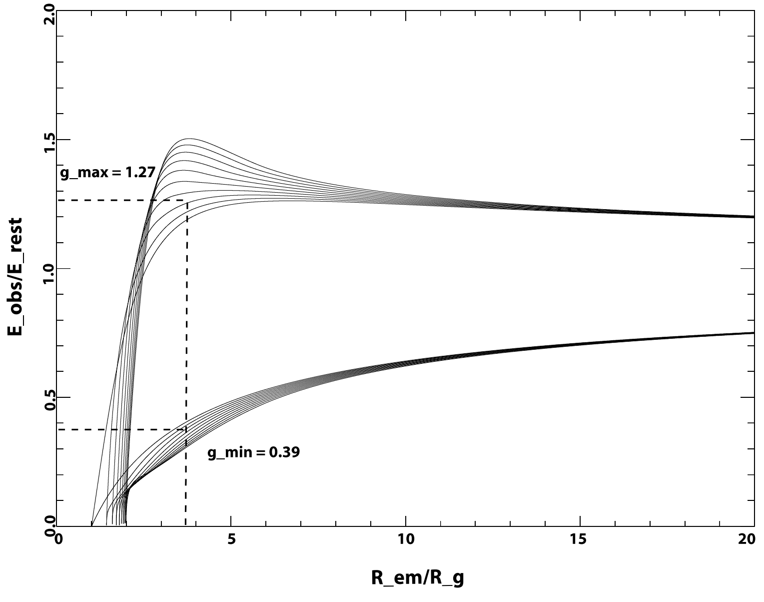

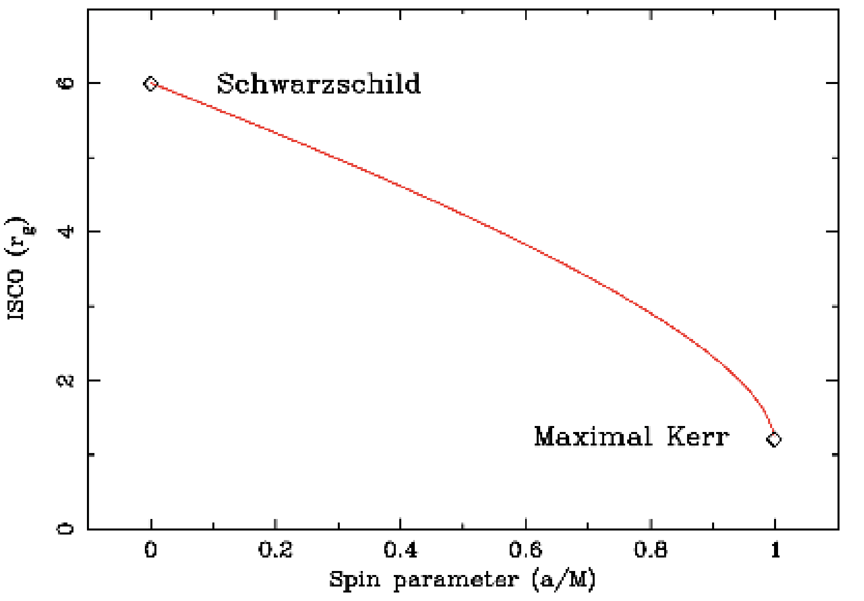

Extremal shifts of the Fe Kα line energy in HE 0435 imply $3r_g < r_{ISCO} < 4r_g$

Conclusions

- Redshifted and blueshifted **Fe lines** with equivalent widths between 500-3000 eV are detected in lensed quasars RXJ1131, QJ0158, HE 0435 and SDSS1004. We interpret these energy shifts as the **result of microlensing of accretion disk** emission within ~ 20 r_g of the black hole.

- For RXJ1131 we find $\boldsymbol{i > 64°}$ and $\mathbf{r_{ISCO} < 8.5r_g}$.

- For HE 0435 we find $\mathbf{3r_g < r_{ISCO} < 4r_g}$

- Several spectra show two shifted Fe lines (**doubles**). Our numerical simulations roughly reproduce the observable results.

- We find that the separation of the peak energies is strongly dependent on spin. The observed ΔE~3 keV constraints $a > 0.8$ for RXJ1131.

- The next step is to fit the results from the simulations to the *Chandra* data and explore the dependence of the results on corona properties.

COLLEGE of CHARLESTON

Future Plans

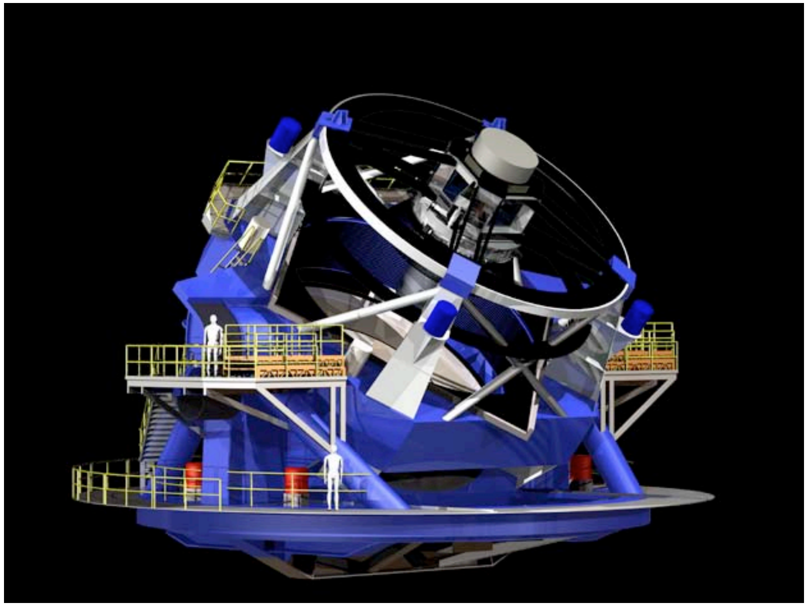

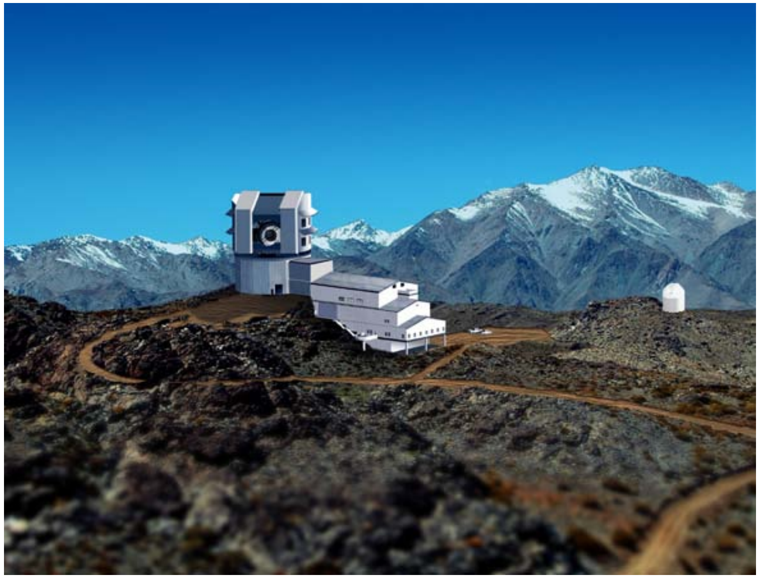

The Large Synoptic Survey Telescope (LSST) will discover ~ 4000 gravitationally lensed quasars that will allow:

- Statistical studies of AGN accretion disk sizes as a function of black hole mass
- Studies of the evolution of AGN disk sizes with redshift
- Studies of the evolution of the mass-to-light ratio of the lens galaxies with redshift
- Studies of the mean stellar mass in cosmologically distant galaxies.

COLLEGE of CHARLESTON